Cavity-induced damping and level shifts in a wide aperture spherical resonator

J.-M. Daul and P. Grangier[a]

Laboratoire Charles Fabry de l'Institut d'Optique, 91403 Orsay Cedex, France

Abstract. We calculate explicitly the space dependence of the radiative relaxation rates and associated level shifts for a dipole placed in the vicinity of the center of a spherical cavity with a large numerical aperture and a relatively low finesse. In particular, we give simple and useful analytic formulas for these quantities, that can be used with arbitrary mirrors transmissions. The vacuum field in the vicinity of the center of the cavity is actually equivalent to the one obtained in a microcavity, and this scheme allows one to predict significant cavity QED effects.

PACS. 32.80.Lg Mechanical effects of light on atoms, molecules, and ions – 32.80.Pj Optical cooling of atoms; trapping – 42.50.Pq Cavity quantum electrodynamics; micromasers – 42.50.Lc Quantum fluctuations, quantum noise, and quantum jumps

1 Introduction

Many theoretical and experimental work has been devoted during recent years to the so-called "cavity QED" regime, where strong coupling is achieved between a few atoms and a field mode contained inside a microwave or optical cavity. In particular, it has been demonstrated that the spontaneous emission rate of an atom inside the cavity is different from its value in free space [1–12]. This effect can be discussed from several different approaches, and here it will be basically attributed to a change of the spectral density of the modes of the vacuum electromagnetic field, which is due to the cavity resonating structure. This approach is particularly convenient when the cavity does not have one single high-finesse mode, but rather many nearly degenerate modes, as it is the case in confocal or spherical cavities. More precisely, we will show that a "wide aperture" concentric resonator using spherical mirrors with a large numerical aperture, can in principle change significantly the spontaneous emission rate even with moderate finesse. Similar result were already demonstrated, using either a spherical cavity [7,11] or "hour-glass" modes in a confocal cavity [12]. In such experiments, the dipole has to sit within the active region volume, which is usually of very small size (of order $(10\lambda)^3$ to $(100\lambda)^3$). In references [11,12], a possible solution was implemented by reducing the cavity finesse in order to have an extended area in which a spherical wave is "self-imaged" on itself. However, getting large effects will put more severe constraints both on the quality of the cavity and on the localisation of the dipoles.

A good understanding of these effects requires first to know the full space dependence of the cavity-induced damping and level shifts. In this paper, we will look at the situation where an atomic dipole lies close to the center of a spherical cavity with a large numerical aperture. We will show that large changes both in the atom damping rate and in its energy levels can be expected, even with a moderate cavity finesse, provided that the atom sits (relatively, but not extremely) close to the cavity center. In the following, we will assume that the cavity damping rate κ is much larger than the free-space atom damping rate γ_{vac}. In that case, the cavity still acts as a continuum with respect to the atomic relaxation, and the damping rate and level shift of an atom at point $\mathbf{r}$ are given by [13]:

$$\Gamma(\mathbf{r}) = \frac{2\pi}{\hbar^2} \sum_k (\mathbf{d} \cdot \mathbf{e}_k(\mathbf{r}))^2 \delta(\omega_k - \omega_o) \tag{1}$$

$$\Delta(\mathbf{r}) = \sum_k \frac{(\mathbf{d} \cdot \mathbf{e}_k(\mathbf{r}))^2}{\hbar^2} \mathcal{P}\left(\frac{1}{\omega_k - \omega_o}\right) \tag{2}$$

where the summation are taken over a complete set of modes denoted by the index k. The resonance frequency and field at point $\mathbf{r}$ for mode k are respectively denoted ω_k and $\mathbf{e}_k(\mathbf{r})$, while the atom resonance frequency and dipole are respectively ω_o and $\mathbf{d}D$, where D is a dimensionless combination of raising and lowering atomic operators. We note that the free-space value of $\Delta(\mathbf{r})$ is a diverging quantity, which is usually assumed to be absorbed in the definition of the atomic levels; therefore, one considers here only the (finite) change of $\Delta(\mathbf{r})$ with respect to this free-space value, that will be denoted $\Delta'(\mathbf{r})$:

$$\Delta'(\mathbf{r}) = \Delta_{\text{cav}}(\mathbf{r}) - \Delta_{\text{vac}}(\mathbf{r}). \tag{3}$$

[a] e-mail: philippe.grangier@iota.u-psud.fr

The purpose of this paper is to present an explicit calculation of $\Delta'(\mathbf{r})$ and $\Gamma(\mathbf{r})/2$, or equivalently of the modification of the (3-D) vacuum modes spectral density due to the presence of the cavity. For definitiveness, we will consider the case of an "open" spherical cavity, of radius R and of reflectivity and transmittivity coefficients r and t, with $r^2 + t^2 = 1$. The cavity can be "open" in the sense that it is made of two separate concentric mirrors which do not cover all 4π steradians. We will assume that $kR \gg 1$ (typically $kR = 10^5$ with $k = \omega/c$), and a moderate cavity finesse (in the range 10–100). These parameters seems accessible from an experimental point of view, and we will show in the next sections that they allow one to get quite significant cavity-induced effects.

2 Modes of a large aperture concentric cavity

We shall first consider the formal case of a scalar field, before turning to the real transverse electromagnetic field. Following the ideas of scattering theory, we propose a computation scheme where the propagation equations are cast in a form that is suitable for the determination of the mode structure and that allows a convenient ray-optics formulation.

2.1 Propagation of a scalar field

We look for stationary solutions $\phi(\mathbf{r}, t) = \phi(\mathbf{r})e^{-i\omega t}$ of

$$\Delta\phi - \frac{1}{c^2}\partial_{tt}^2\phi = 0 \tag{4}$$

that is, in spherical coordinates (r, θ, ϕ)

$$\frac{1}{r}\partial_{rr}^2(r\phi) + k^2\phi + \frac{1}{r^2}\Delta_s\phi = 0 \tag{5}$$

where we note $k = \omega/c$ and introduce the spherical Laplacian

$$\Delta_s = \frac{1}{\sin^2\theta}\partial_{\phi\phi}^2 + \partial_{\theta\theta}^2 + \frac{\cos\theta}{\sin\theta}\partial_\theta \tag{6}$$

with eigenvalues $-l(l+1), l \geq 0$.

In the far-field regime: $r \rightarrow \infty$, we can write unambiguously

$$\phi(\mathbf{r} = r\hat{\mathbf{\Omega}}) = \frac{e^{ikr}}{r}f_r^{\text{out}}(\hat{\mathbf{\Omega}}) + \frac{e^{-ikr}}{r}f_r^{\text{in}}(\hat{\mathbf{\Omega}}). \tag{7}$$

In the following we will often omit the argument $\hat{\mathbf{\Omega}}$ of $f^{\text{out,in}}$. The quantity $f_r^{\text{out,in}}$ depend slowly on r: $\partial_r f_r^{\text{out,in}} \sim f_r^{\text{out,in}}/r$ and tend to large r angular distributions:

$$f_r^{\text{out,in}} \xrightarrow[r\to\infty]{} f_\infty^{\text{out,in}}. \tag{8}$$

Such an 'out' field occurs for instance in the case of a radiating localized source: its squared amplitude then corresponds to the power radiated along $\hat{\mathbf{\Omega}}$ per unit solid angle. Here we also allow for incoming radiation, focused on a localized region — which, if not absorbed, turns after focusing into outgoing radiation. Note that this separation in 'in' and 'out' field is not possible too close to the origin, when the Poynting vector is no more almost radial.

2.1.1 Far-field solution

We have separate propagation equations for $f_r^{\text{out,in}}$: the 'in' field obeying

$$\partial_r f_r + \frac{i}{2k}\partial_{rr}^2 f_r + \frac{i}{2kr^2}\Delta_s f_r = 0. \tag{9}$$

Defining $\delta f = f_r - f_\infty$ we obtain

$$\partial_r \delta f = \frac{-i}{2kr^2}\Delta_s f_\infty - \frac{i}{2kr^2}\Delta_s \delta f - \frac{i}{2k}\partial_{rr}^2\delta f$$

with orders $\quad \frac{\delta f}{r} \qquad \frac{f_\infty}{kr^2} \qquad\qquad \frac{\delta f}{kr^2} \qquad\qquad \frac{\delta f}{kr^2}$ (10)

(we are only interested in the large r asymptotics, so we first ignore Δ_s to get the orders of the different terms).

The first term in the r.h.s. gives the leading behaviour

$$\delta f \simeq \frac{i}{2kr}\Delta_s f_\infty \tag{11}$$

and a systematic expansion can be obtained by solving iteratively (10) producing terms

$$\frac{\Delta_s^n}{(kr)^{n+p}}f_\infty, \quad \begin{cases} n \geq 1 \\ p \geq 0 \end{cases}. \tag{12}$$

In the sequel, we shall be interested in the field at $\sim 100\lambda$ off the origin: in geometric optics this involves light-rays with an impact parameter smaller than 100λ, or photons with orbital angular momentum smaller than $100\hbar$. Therefore, in the multipole expansion of the field, we only keep harmonics with $l \leq 100$: Δ_s is now at most of the order 10^4. Using our typical value $kR \simeq 10^5$, the terms (12) with $p \geq 1$ are then negligible, and all $p = 0$ terms are obtained by neglecting the last term in (10), which is equivalent to replacing (9) with

$$\partial_r f_r = \frac{-i}{2kr^2}\Delta_s f_r \tag{13}$$

Its solution

$$f_r = e^{i\Delta_s/2kr}f_\infty \tag{14}$$

then gives all the $p = 0$ terms of the expansion (12). It is easy to show that with $\Delta_s \sim 10^4$, $kr \sim 10^5$ the magnitude of this first term is a few percent, while the next two terms range as 10^{-7}. Therefore, we shall use only the first term $f_r^{\text{in}} = e^{\frac{i\Delta_s}{2kr}}f_\infty^{\text{in}}$ in the following.

To conclude this section, we extend these results to the case of outgoing waves: so far we only considered incoming radiation, but the analogue of (9) is simply given by changing i to $-i$, and all results are easily transposed under complex conjugation, as an example of time reversal. In particular, we shall use

$$f_r^{\text{out}} = e^{-\frac{i\Delta_s}{2kr}}f_\infty^{\text{out}}. \tag{15}$$

2.1.2 Solution at any distance

Up to now, we only studied asymptotic expansions of solutions of the wave equation in spherical coordinates, expressing $f_r(\hat{\mathbf{\Omega}})$ for large r in terms of the values taken by f_∞ in the neighbourhood of $\hat{\mathbf{\Omega}}$. We will now derive an integral equation giving f_r at any finite distance in terms of the function f_∞.

In the case of a stationary wave propagating in free space (with sources at infinity), we expect the knowledge of f_∞^{in} to enable us to determine the solution $\phi(\mathbf{r})$ everywhere, and in particular its asymptotic behaviour f_∞^{out}: forming wave-packets, this amounts to constructing the solution at any time, given its value in the infinite past. We claim that the exact solution is obtained by a sum of plane waves

$$\phi(\mathbf{r}) = -2ik \int \frac{d\hat{\mathbf{\Omega}}}{4\pi} f_\infty^{\text{in}}(\hat{\mathbf{\Omega}}) e^{i(-k\hat{\mathbf{\Omega}})\mathbf{r}} \tag{16}$$

$f_\infty^{\text{in}}(\hat{\mathbf{\Omega}})$ being the amplitude of the wave coming from direction $\hat{\mathbf{\Omega}}$ with wave-vector $-k\hat{\mathbf{\Omega}}$.

Obviously, the proposed solution does satisfy the wave equation, as a superposition of plane-waves; to prove our statement it thus suffices to verify that (16) has the right asymptotic behaviour f_∞^{in}. But for large r the integral is dominated by its points of stationary phase; suppose, for definiteness, that the axis $\theta = 0$ is in the direction of $\mathbf{r}$: then the phase in (16) $-ikr\cos\theta$ is stationary at $\theta = 0$ and $\theta = \pi$. Near each of these points, the leading contribution to the integral will be of order $1/kr$, with corrections corresponding to higher powers of $1/kr$: so, the asymptotic part $\phi^{\text{in,out}}$ is entirely determined by the leading contribution to the integral. Using

$$\int_{\text{near }\theta=0} d\hat{\mathbf{\Omega}}\, e^{-iA\cos\theta} \underset{A\to\infty}{\simeq} \frac{2i\pi}{A} e^{-iA} \tag{17}$$

we obtain the contributions of neighbourhoods of $\theta = 0$ and $\theta = \pi$ to $\phi(\mathbf{r})$

$$\frac{e^{-ikr}}{r} f_\infty^{\text{in}}(\theta = 0); \quad -\frac{e^{ikr}}{r} f_\infty^{\text{in}}(\theta = \pi) \tag{18}$$

corresponding respectively to the 'in' and 'out' fields, as could easily have been figured out.

We recognize the right 'in'-field in this expansion, and have proved the validity of (16). Moreover, we have obtained the following relation between 'in' and 'out' fields

$$f_\infty^{\text{out}}(\hat{\mathbf{\Omega}}) = -f_\infty^{\text{in}}(-\hat{\mathbf{\Omega}}). \tag{19}$$

If a wave is focused, it emerges in the opposite direction, with the opposite phase. We also recognize in the i factor in the integral:

$$\phi(\mathbf{r}) = \frac{-i}{\lambda} \int d\hat{\mathbf{\Omega}} f_\infty^{\text{in}}(\hat{\mathbf{\Omega}}) e^{i(-k\hat{\mathbf{\Omega}})\mathbf{r}} \tag{20}$$

the relative $\pi/2$ phase at the focus point.

Corrections to this leading behaviour will produce the asymptotic expansion of $f_r^{\text{in,out}}$ in powers of $1/kr$, the neighbourhood of $\theta = 0$ contributing to f_r^{in} and that of $\theta = \pi$ to f_r^{out}. In this way, one can recover, with longer calculations, the results of the preceding section. For instance, including the first correction to f_r^{in} amounts to replacing $f_\infty^{\text{in}}(\theta = 0)$ with $f_\infty^{\text{in}}(0) + i/2kr\, (\Delta_s f_\infty^{\text{in}})(0)$.

2.1.3 A complete set of explicit solutions

We know that the angular distribution of the field has variations with r given by an operator expressed with Δ_s: thus, eigenfunctions of Δ_s — spherical harmonics — give r-independent angular distributions (up to normalization and phase), that is, factorized solutions:

$$Y_{lm}(\hat{\mathbf{\Omega}})j(r). \tag{21}$$

The wave equation and the smoothness of the solution at $r = 0$ then determine $j(r)$ up to a constant factor:

$$j(r) = \frac{J_{l+1/2}(kr)}{\sqrt{kr}}. \tag{22}$$

Using the asymptotics of Bessel functions

$$\frac{J_{l+1/2}(kr)}{\sqrt{kr}} \underset{r\to\infty}{=} \sqrt{\frac{2}{\pi}} \frac{1}{kr} \sin\left(kr - \frac{\pi l}{2} + \frac{l(l+1)}{2kr}\right) + \mathcal{O}\left(1/r^3\right) \tag{23}$$

we obtain the large r behaviour of this explicit solution

$$\phi(\mathbf{r} = r\hat{\mathbf{\Omega}}) = -2ik(-i)^l \sqrt{\frac{\pi}{2}} Y_{lm}(\hat{\mathbf{\Omega}}) \frac{J_{l+1/2}(kr)}{\sqrt{kr}}$$
$$= \left[Y_{lm}(\hat{\mathbf{\Omega}}) \frac{e^{-ikr}}{r} e^{-i\frac{l(l+1)}{2kr}} \right.$$
$$\left. - (-1)^l Y_{lm}(\hat{\mathbf{\Omega}}) \frac{e^{-ikr}}{r} e^{i\frac{l(l+1)}{2kr}} + \mathcal{O}\left(1/r^2\right) \right]. \tag{24}$$

We can verify in this particular case the general relation $f_\infty^{\text{out}}(\hat{\mathbf{\Omega}}) = -f_\infty^{\text{in}}(-\hat{\mathbf{\Omega}})$ and check the action of $\exp i\Delta_s/2kr$ on f_∞^{in} to the accuracy of (24).

We can also check the expression for the field at finite distance (16): noting that $f_\infty^{\text{in}} = Y_{lm}$ and choosing normalized spherical harmonics

$$\langle Y_{lm} \mid Y_{lm} \rangle = \int \frac{d\hat{\mathbf{\Omega}}}{4\pi} |Y_{lm}|^2 = 1 \tag{25}$$

we decompose

$$f_\infty^{\text{in}} = \sum_{lm} \langle Y_{lm} \mid f_\infty^{\text{in}} \rangle Y_{lm} \tag{26}$$

and obtain

$$\phi(r\hat{\mathbf{\Omega}}) =$$
$$\sum_{lm} \langle Y_{lm} \mid f_\infty^{\text{in}} \rangle \frac{-2ik}{i^l} \sqrt{\frac{\pi}{2}} Y_{lm}(\hat{\mathbf{\Omega}}) \frac{J_{l+1/2}(kr)}{\sqrt{kr}}. \tag{27}$$

The rotationally invariant quantity $\sum_m \overline{Y_{lm}(\hat{\boldsymbol{\Omega}})} Y_{lm}(\hat{\boldsymbol{\Omega}}')$ is conveniently evaluated when the axis of reference is chosen along $\hat{\boldsymbol{\Omega}}$ and has value $(2l+1)P_l(\cos\alpha)$, P_l being the lth Legendre polynomial, and α the angle between $\hat{\boldsymbol{\Omega}}$ and $\hat{\boldsymbol{\Omega}}'$. Using the formula

$$\sum_{l\geq 0} i^l \frac{J_{l+1/2}(kr)}{\sqrt{kr}}(2l+1)P_l(\cos\alpha) = \sqrt{\frac{2}{\pi}} e^{ikr\cos\alpha} \quad (28)$$

we finally obtain

$$\phi(\mathbf{r}) = \left\langle 2ike^{ik\hat{\boldsymbol{\Omega}}'\mathbf{r}} \mid f_\infty^{\mathrm{in}}(\hat{\boldsymbol{\Omega}}') \right\rangle_{\hat{\boldsymbol{\Omega}}'} \quad (29)$$

which reproduces (16).

2.2 Modes of concentric cavities

2.2.1 Perfect spherical resonator

The explicit solutions given above allow us to determine the field modes inside a perfectly reflecting sphere, with radius $R \gg \lambda$: when we classify modes according to their spherical symmetry (quantum numbers l, m), the requirement that the field shall vanish on the inner face of the cavity

$$f_R = f_R^{\mathrm{in}} e^{-ikR} + f_R^{\mathrm{out}} e^{ikR} = 0 \quad (30)$$

reads $J_{l+1/2}(kR) = 0$, or according to (23):

$$kR - \frac{\pi}{2}l + \frac{l(l+1)}{2kR} = 0 \qquad [\mathrm{mod}\ \pi] \quad (31)$$

for the mode l, m, where we have written all significant terms for $l \sim 100$; $kR \sim 10^5$, obtaining by the way the lowest order for which the l-degeneracy is disproved. The eigenfrequencies are then

$$\nu_{l,n} = \frac{kc}{2\pi} = \frac{c}{2R}\left(n + \frac{l}{2} - \frac{l(l+1)}{2\pi kR}\right) \quad (32)$$

n being the number of radial nodes.

With our numerical values the l-frequency shift has relative magnitude which is up to $l/2\pi kR \sim 2\times 10^{-4}$, and is therefore very small compared to the cavity linewidth. We note that at a point close to the center, small l modes are more important, since photons travelling close to the origin carry a small orbital momentum. This point will be made quantitative later, when we will discuss the case of a spherical cavity with finite transmission.

2.2.2 Modes in an open cavity

Principle of the determination of the mode structure

We recognize the vacuum fluctuations in a concentric cavity as induced by the vacuum fluctuations of the outer void space which enter into the cavity: we will thus start our analysis by studying how any incident radiation can enter in the open concentric resonator.

We consider two spherical mirrors, facing each other in vacuum, with common center O — as if in the preceding example the tropical zone of the sphere were transparent, while the polar zones remained coated. For our computation, we shall replace the infinite vacuum with the inner volume of a very large sphere centered at O, thus replacing a true continuum with a discrete series of very closely spaced lines. We will use $\mathcal{R}$ to denote the radius of the outer closed sphere, and R for the inner sphere, partially covered by mirrors; and use the following notation for the field of an eigenmode

$$\mathcal{R} > r > R: \quad \frac{1}{r}e^{ikr}f_r^{\mathrm{out}} + \frac{1}{r}e^{-ikr}f_r^{\mathrm{in}}$$
$$R > r: \quad \phi(\mathbf{r}). \quad (33)$$

Note that the decomposition between 'in' and 'out' fields in the first equation is allowed by our choice to study only modes which contribute to ϕ near O, that is, not too unfocused.

We can formally extend ϕ for larger values of r as if there were no cavity at all, and write the far-field decomposition

$$\frac{1}{r}e^{ikr}g_r^{\mathrm{out}} + \frac{1}{r}e^{-ikr}g_r^{\mathrm{in}} \quad (34)$$

g_∞^{in} is the incoming radiation which induces in void space the same field near O as f_∞^{in} does in the presence of mirrors. We are ensured that $g_\infty^{\mathrm{out}}(\hat{\boldsymbol{\Omega}}) = -g_\infty^{\mathrm{in}}(-\hat{\boldsymbol{\Omega}})$ since that field propagates through the origin. However, the same equality does not hold for f: to understand the relation between f^{in} and f^{out}, we note that the incoming radiation f^{in} induces a field in the open cavity, which in turn (perhaps after resonance) emits an outgoing field f^{out}; writing the precise relation would require to solve the propagation equation for $r > R$, write the boundary conditions on the mirrors, and obtain the condition on $f^{\mathrm{in,out}}$ for the existence of a solution ϕ between the mirrors satisfying $g_\infty^{\mathrm{out}}(\hat{\boldsymbol{\Omega}}) = -g_\infty^{\mathrm{in}}(-\hat{\boldsymbol{\Omega}})$. In some sense, g directly goes through the origin, while f^{in} turns into f^{out} after reflection on the mirrors, or multiple reflections in the cavity. We will not try to write any explicit formula for that, but use some general properties of the relation

$$f_\infty^{\mathrm{in}} \mapsto f_\infty^{\mathrm{out}} = \hat{S} f_\infty^{\mathrm{in}} \quad (35)$$

in close analogy to scattering theory.

We will assume that the losses on the mirrors are negligible when compared to the transmittivity: the balance between the incoming and outgoing energy fluxes

$$\left\| f_\infty^{\mathrm{out}} \right\|^2 = \left\| f_\infty^{\mathrm{in}} \right\|^2 = \int \frac{d\hat{\boldsymbol{\Omega}}}{4\pi} \left| f_\infty^{\mathrm{in}} \right|^2 \quad (36)$$

requires $\hat{S}$ to be unitary.

We now express the condition of perfect reflection on the inner face of the large closed cavity, i.e. that the field vanishes for $r = \mathcal{R}$:

$$e^{ik\mathcal{R}} f_\mathcal{R}^{\mathrm{out}} + e^{-ik\mathcal{R}} f_\mathcal{R}^{\mathrm{in}} = 0. \quad (37)$$

Once again, we are interested only in those modes that are focused enough so that they may contribute to the field near O: l being bounded, if $\mathcal{R}$ is large enough we may use $f_{\mathcal{R}} \simeq f_{\infty}$ and rewrite the preceding formula

$$\hat{S} f_{\infty}^{\text{in}} = -e^{-2ik\mathcal{R}} f_{\infty}^{\text{in}} \tag{38}$$

and formulate the problem of determining the modes of the open cavity (enclosed in a large one) as follows: find a wavenumber k such that $-e^{-2ik\mathcal{R}}$ is an eigenvalue of the unitary operator $\hat{S}_k$ and identify the corresponding eigenvector. We precised our notation and used $\hat{S}_k$ to make clear the dependency of the scattering operator on the frequency at which the open cavity is excited. However, the problem is not so intricated since $\hat{S}_k$ depends slowly on k on the scale of the free spectral range of the $\mathcal{R}$-cavity:

$$\delta k\, R \mathcal{F} \ll 1 \;\Rightarrow\; \hat{S}_k \simeq \hat{S}_{k+\delta k} \tag{39}$$

with $\mathcal{F}$ the finesse of the R-cavity. So, in order to find the eigenmodes with wavenumbers $k \simeq k_0$ we have to find the eigenvalues and eigenvectors of $\hat{S}_{k_0}$; then adjust k so that $-e^{-2ik\mathcal{R}}$ coincides with any chosen eigenvalue of $\hat{S}_{k_0}$. Clearly, the mode structure so obtained will be (locally) periodic: the same eigenvector of $\hat{S}_{k_0}$ occuring as the far-field of a mode every $\delta k = \pi/\mathcal{R}$ or $\delta \nu = c/2\mathcal{R}$.

We would like to stress the close analogy between this general scheme and scattering theory. The operator $\hat{S}$ is to be thought of as an S-matrix in interaction representation: indeed, we can actually take the limit of large r for the connection between f_r^{in} and f_r^{out}, but not for the relation between $e^{-ikr} f_r^{\text{in}}$ and $e^{ikr} f_r^{\text{out}}$. Following our analogy, we may say that the radial propagation with phase factor e^{ikr} corresponds to free evolution in perturbation theory, while the orthoradial propagation of light with changes in the angular distribution f corresponds to the perturbation and asymptotically vanishes (at large r vs. at large times in scattering theory).

Normalization of the modes

We define the total energy of the field to be $\int d^3\mathbf{r}\, |\phi(\mathbf{r})|^2 = 2\int d^3\mathbf{r}\, \widehat{\phi_{\text{real}}^2}^{\text{time}}$ where $\phi_{\text{real}}(\mathbf{r}, t) = \text{Re}[\phi(\mathbf{r})e^{-i\omega t}]$. For large enough $\mathcal{R}$ this energy integral is dominated by large r regions where we can approximate

$$\phi(\mathbf{r}) \simeq \frac{1}{r} e^{ikr} f_{\infty}^{\text{out}} + \frac{1}{r} e^{-ikr} f_{\infty}^{\text{in}} \tag{40}$$

and so obtain for the energy

$$\mathcal{E} = 4\pi\,\mathcal{R}\,\left(\left\| f_{\infty}^{\text{in}} \right\|^2 + \left\| f_{\infty}^{\text{out}} \right\|^2 \right) = 8\pi\,\mathcal{R}\,\left\| f_{\infty}^{\text{in}} \right\|^2. \tag{41}$$

We decide to call vacuum the state in which every mode is excited with energy 1 (in real electrodynamics we should use $\hbar\omega/2$) so that the normalization of any mode in vacuum is

$$\left\| f_{\infty}^{\text{in}} \right\|_{\text{vac}}^2 = \frac{1}{8\pi\mathcal{R}}. \tag{42}$$

We can easily express the fluctuations of the ordinary vacuum field (here, ordinary means in infinite space) or rather their spectral density: in a range of frequencies $\delta\nu$ we have

$$\frac{V}{(2\pi)^3} \int_{\delta\nu} d^3\mathbf{k} = \frac{4\pi V}{c^3} \nu^2\, \delta\nu \tag{43}$$

modes for the case of a large volume V with periodic boundary conditions, while each mode contributes $1/V$ to $|\phi(\mathbf{r})|^2$ since the energy of any mode is uniformly distributed in the volume. Finally, one has the expected result in ordinary vacuum:

$$\left\langle |\phi(\mathbf{r})|^2 \right\rangle_{\delta\nu} = \frac{4\pi}{c^3} \nu^2\, \delta\nu. \tag{44}$$

In the next part, we will derive an analogous formula for the case of an open concentric cavity and compute by how much the vacuum fluctuations (near the center) are amplified or reduced by the presence of mirrors at about 1 cm. Before that, a last comment is in order: to obtain the above expression for the ordinary vacuum field we used the fact that the contributions of different modes add up incoherently. This is always true when we use a basis of modes in which the energy operator (Hamiltonian of the field) is diagonal: in general, eigenmodes are non-degenerate in frequency and this condition is automatically satisfied. This vanishing of the off-diagonal matrix elements of the energy reads

$$\int d^3\mathbf{r}\, \phi_1^*(\mathbf{r})\, \phi_2(\mathbf{r}) = 0 \tag{45}$$

and expresses the orthogonality of different modes with respect to volume integral.

The discussion of the preceding part enables us to assert a more precise property, which will be essential in the following: even the angular overlap of different modes is 0. Indeed, we argued that eigenmodes were obtained by diagonalizing the unitary operator $\hat{S}_{k_0}$: but evidently, two different eigenfunctions of the same unitary operator are orthogonal. Thus, the far-fields of different modes have a vanishing angular overlap, unless the two particular modes do have the same far-field asymptotics: in the latter case, their number of radial nodes being different ensures the vanishing of their volume overlap.

That property can be stated differently: if we consider all eigenmodes in a range of frequencies $\delta\nu = c/2\mathcal{R}$ and associate to every such mode its f_{∞}^{in} we obtain a complete orthogonal set of normalized angular functions. Should we consider a larger range $\delta\nu$ every member of this orthogonal family would then be counted $2\,\mathcal{R}\,\delta\nu\,/c$ times.

Modification of the vacuum field in an open cavity

We will find an expression for the field at points close to the origin ($r <$ a few hundreds $\lambdabar$ that is a few dozens μm). All light rays that pass so close to the center will then reflect almost normally on the mirrors: we will assume that the wave-fronts of all modes are sufficiently tangent to the mirrors for us to use the $i = 0$ reflectivity and transmittivity coefficients ρ, τ ($\rho = 1$ for a perfect mirror).

Let us first compute the field induced in the open cavity by incident radiation $f_\infty^{\rm in}$: we will note $f_r^{\rm in} = U_r f_\infty^{\rm in}$ with $U_r \simeq e^{i\Delta_s/2kr}$ according to our previous results. A similar relation holds for 'out' fields with $\bar{U}_r = U_r^+$ or U_r^{-1} since U_r is (almost) unitary. On the outer face of the mirror, the field has incoming and outgoing amplitudes

$$\frac{e^{-ikR}}{R} U_R f_\infty^{\rm in}, \quad \frac{e^{ikR}}{R} \bar{U}_R f_\infty^{\rm out} \qquad (46)$$

while on the inner face we find

$$\frac{e^{-ikR}}{R} U_R g_\infty^{\rm in}, \quad \frac{e^{ikR}}{R} \bar{U}_R g_\infty^{\rm out} \qquad (47)$$

with

$$g_\infty^{\rm out}(\hat{\mathbf{\Omega}}) = -g_\infty^{\rm in}(-\hat{\mathbf{\Omega}}): \quad g_\infty^{\rm out} = -\hat{P} g_\infty^{\rm in} \qquad (48)$$

$\hat{P}$ being the parity operator, that commutes with Δ_s and U_R. The $g^{\rm in}$ wave has two contributions: partial transmission of $f^{\rm in}$ and partial reflection of $g^{\rm out}$:

$$e^{-ikR} U_R\, g_\infty^{\rm in}(\hat{\mathbf{\Omega}}) = -\rho(\hat{\mathbf{\Omega}}) e^{ikR} \bar{U}_R\, g_\infty^{\rm out}(\hat{\mathbf{\Omega}})$$
$$+ \tau(\hat{\mathbf{\Omega}}) e^{-ikR} U_R\, f_\infty^{\rm in}(\hat{\mathbf{\Omega}}) \quad (49)$$

where we explicitly write the angular dependency of ρ, τ: in particular, out of the mirrors $\rho = 0$ and $\tau = 1$. We can easily solve (48, 49) to obtain

$$g_\infty^{\rm in}(\hat{\mathbf{\Omega}}) = U_R \frac{1}{U_R^2 - e^{2ikR}\rho(\hat{\mathbf{\Omega}})P}\tau(\hat{\mathbf{\Omega}}) U_R\, f_\infty^{\rm in}(\hat{\mathbf{\Omega}}) \qquad (50)$$

which yields a formula for the field at any point through

$$\phi(\mathbf{r}) = \left\langle 2ike^{ik\hat{\mathbf{\Omega}}\mathbf{r}} \mid g_\infty^{\rm in}(\hat{\mathbf{\Omega}}) \right\rangle_{\hat{\mathbf{\Omega}}}. \qquad (51)$$

Introducing the shorter notation

$$\mathcal{T} = \tau(\hat{\mathbf{\Omega}}) \frac{1}{U_R^2 - e^{2ikR}P\rho(\hat{\mathbf{\Omega}})} U_R \qquad (52)$$

we obtain for the vacuum field

$$\left\langle |\phi(\mathbf{r})|^2 \right\rangle_{\rm vac} = \sum_{\text{modes: } f_\infty^{\rm in}} \left\langle 2ike^{ik\hat{\mathbf{\Omega}}\mathbf{r}} \left| \bar{\mathcal{T}}^+ U_R \right| f_\infty^{\rm in} \right\rangle$$
$$\times \left\langle f_\infty^{\rm in} \left| U_R^+ \bar{\mathcal{T}} \right| 2ike^{ik\hat{\mathbf{\Omega}}\mathbf{r}} \right\rangle. \quad (53)$$

The above-mentioned property of orthogonality of the modes now gives a considerable simplification since we do not need to know the precise expression of all the modes, but only their total contribution to the physically meaningful quantity $\langle |\phi(\mathbf{r})|^2 \rangle_{\rm vac}$ in a given frequency range: so, no matter what the true $f_\infty^{\rm in}$ may look like, they surely give a closure relation. Recalling that the $f_\infty^{\rm in}$ associated

to the modes in a frequency range of $c/2\mathcal{R}$ form a complete orthogonal set normalized according to (42) we see that

$$\sum_{\text{modes in } \delta\nu:\, f_\infty^{\rm in}} |f_\infty^{\rm in}\rangle\langle f_\infty^{\rm in}| = \frac{2\mathcal{R}\,\delta\nu}{c}\frac{1}{8\pi\mathcal{R}}\,\mathbf{1} \qquad (54)$$

and is actually independent of the large cavity we used to mimic the infinite vacuum. We then have

$$\left\langle |\phi(\mathbf{r})|^2 \right\rangle_{\rm vac} = \frac{k^2\,\delta\nu}{\pi c}\left\| U_R^+\,\bar{\mathcal{T}}\, e^{ik\hat{\mathbf{\Omega}}\mathbf{r}} \right\|^2. \qquad (55)$$

Using the unitarity of U_R and the expression of ordinary vacuum fluctuations we find

$$\frac{\left\langle |\phi(\mathbf{r})|^2 \right\rangle_{\rm cav}}{\left\langle |\phi(\mathbf{r})|^2 \right\rangle_{\rm vac}} = \left\| \mathcal{T}\, e^{-ik\hat{\mathbf{\Omega}}\mathbf{r}} \right\|^2$$
$$= \left\| \tau \frac{1}{e^{i\Delta_s/kR} - e^{2ikR}P\rho} e^{i\Delta_s/2kR}\, e^{-ik\hat{\mathbf{\Omega}}\mathbf{r}} \right\|^2. \quad (56)$$

### 2.2.3 Numerical study and ray optics interpretation

Numerical results

As expressed in (56), we shall evaluate the action of an operator on the function $\hat{\mathbf{\Omega}} \mapsto e^{-ik\hat{\mathbf{\Omega}}\mathbf{r}}$ and then compute the squared norm of the resulting function: this can be done numerically, decomposing functions on spherical harmonics

$$e^{-ik\hat{\mathbf{\Omega}}\mathbf{r}} = \sum_{l,m;\, 0\le|m|\le l} (-i)^l \sqrt{\frac{\pi}{2}}\frac{J_{l+1/2}(kr)}{\sqrt{kr}}$$
$$\times \overline{Y_{l,m}\,(\mathbf{r}/r)}\, Y_{l,m}(\hat{\mathbf{\Omega}}) \quad (57)$$

and computing matrix elements of the k-dependent operator in the basis of spherical harmonics.

We only considered axially-symmetric cavities: in that case, the operators involved conserve m and the result is expressed as a sum of contributions from the different m sectors. Moreover, $m = 0$ gives the single contribution to the field on the axis. In the latter case, we could use truncated systems of up to $l_{\max} = 300$ spherical harmonics and study the effect of truncation: the result was constant within 1% for $l_{\max} \ge 100$. In the general case (field fluctuations at points away from the symmetry axis of the cavity), we used $l_{\max} = 100$ with any m to study the spatial and spectral dependency of vacuum fluctuations.

The graphs shown in Figure 1 were obtained with concentric mirrors of uniform reflectivity $\rho = 0.98$ (giving an intensity transmittivity $T \simeq 4\%$) covering 30% of the 4π steradian; this is obtained for an half-aperture angle $\theta_m = 45°$ for each mirror. The frequency is set at the resonance value at the cavity center. We note the rapid oscillations of the amplitude of vacuum fluctuations near the center of the cavity; right at the center, the obtained value at resonance agrees approximately with the usual
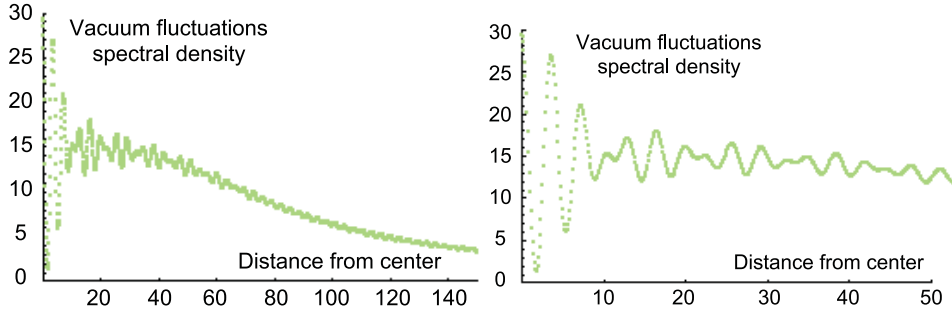
Fig. 1. Spatial variation of vacuum fluctuations on the cavity axis, obtained from a full numerical calculation. The horizontal axis unit is $1/k$, and the vertical axis unit is the standard vacuum level. The amplitude reflection coefficient of the mirrors is taken to be $\rho = 0.98$, and the numerical aperture of the cavity is 0.7. The right hand side of the figure is a zoom close to the cavity center.

rough estimate $4/T \times \Delta\Omega_{\mathrm{mirr}}/4\pi$. However, at a few μm away from the center the enhancement effect is halved, and then decreases further on a scale of $\sim 15\lambda$. The next sections will give support to a qualitative and quantitative formulation of these facts in terms of ray-optics.

Case of a closed cavity: ray optics interpretation

We come back to the case of a closed spherical resonator, now allowing a non-zero transmittivity of the mirrors (but still negligible losses, as we always suppose in this article). We can apply to that particular case the formalism we developed for open cavity, and recover the known modes involving spherical harmonics:

$$\frac{1}{e^{i\Delta_s/kR} - e^{2ikR}P_\rho} e^{i\Delta_s/2kR} Y_{l,m} =$$
$$\frac{1}{e^{-il(l+1)/kR} - (-1)^l\rho e^{2ikR}} e^{-il(l+1)/2kR} Y_{l,m} \quad (58)$$

so that the vacuum fluctuations (normalized to 1 for usual vacuum) read

$$\sum_{l\geq 0} \frac{T}{\left|e^{-il(l+1)/kR} - (-1)^l\rho e^{2ikR}\right|^2} \frac{\pi}{2}(2l+1)\frac{J_{l+1/2}(kr)^2}{kr}$$
$$(59)$$

where we recognize the usual resonance factor, including the slight non-degeneracy of modes (increasing l: lower resonant frequency) and see the explicit spatial-dependency of l-modes.

Averaging vacuum fluctuations in a frequency range much larger than the 'free' spectral interval of the cavity we can replace the frequency-dependent factor by its average value: 1, and use the following sum rule

$$\sum_{l\geq 0} \frac{\pi}{2}(2l+1)\frac{J_{l+1/2}(kr)^2}{kr} = 1. \quad (60)$$

We actually recover usual vacuum if the cavity is large enough (with free spectral range smaller than the experimentally used frequency bandwidth).

If we are interested in the behaviour of vacuum fluctuations in the vicinity of the center (a few microns) where only small l modes contribute, we may assume that all modes are degenerate and use a common resonant factor:

$$\frac{T}{|1 - (-1)^l\rho e^{2ikR}|^2}. \quad (61)$$

The sum rules for Bessel functions

$$\sum_{l:\mathrm{odd/even}} \frac{\pi}{2}(2l+1)\frac{J_{l+1/2}(kr)^2}{kr} = \frac{1}{2} \pm \frac{\sin 2kr}{4kr} \quad (62)$$
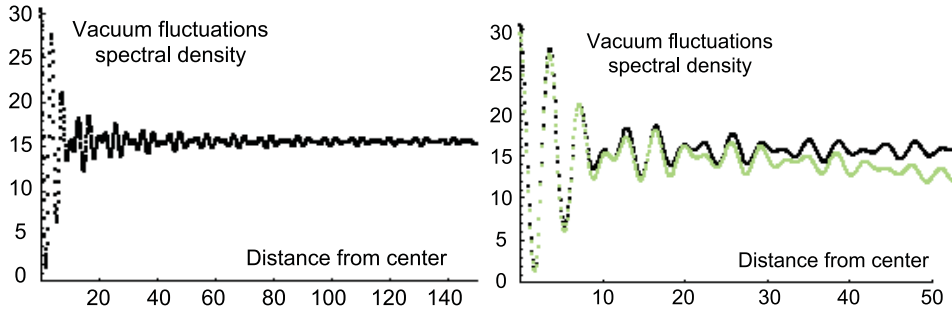
then allow us to write the vacuum field as

$$\frac{T}{|1 - \rho e^{2ikR}|^2}\left(\frac{1}{2} + \frac{\sin 2kr}{4kr}\right)$$
$$+ \frac{T}{|1 + \rho e^{2ikR}|^2}\left(\frac{1}{2} - \frac{\sin 2kr}{4kr}\right). \quad (63)$$

At any point, we have two series of resonant lines, in which the vacuum noise is distributed with weights $1/2 \pm \sin 2kr/4kr$. At a frequency which is resonant for the center of the cavity, the spatial dependency of the vacuum field shows a reduction by a factor 2 when one moves away from the center, as was noted above in the case of an open cavity; we interpret this as the distribution of vacuum fluctuations on the two series of lines: right at the center only the $l = 0$ mode appear, but the odd l modes have no other common nodes and share $\simeq 50\%$ of the vacuum noise away from the center. The same conclusions can be formulated in terms of light-rays: noting that

$$\frac{1}{2} + \frac{\sin 2kr}{4kr} = \int \frac{d\hat{\boldsymbol{\Omega}}}{4\pi}\,\cos^2(k\hat{\boldsymbol{\Omega}}\cdot\mathbf{r}),$$
$$\frac{1}{2} - \frac{\sin 2kr}{4kr} = \int \frac{d\hat{\boldsymbol{\Omega}}}{4\pi}\,\sin^2(k\hat{\boldsymbol{\Omega}}\cdot\mathbf{r}) \quad (64)$$

Fig. 2. Spatial variation of vacuum fluctuations on the cavity axis, obtained from a simple ray-optics calculation. The horizontal axis unit is $1/k$, and the vertical axis unit is the standard vacuum level. The amplitude reflection coefficient of the mirrors is taken to be $\rho = 0.98$, and the numerical aperture of the cavity is 0.7. The right hand side of the figure is a zoom close to the cavity center, which shows also a comparison with the full calculation (Fig. 1).

we may express the vacuum fluctuations (still neglecting the l-dependency of resonant frequencies) as

$$\frac{\left\langle |\phi(\mathbf{r})|^2 \right\rangle_{\text{cav}}}{\left\langle |\phi(\mathbf{r})|^2 \right\rangle_{\text{vac}}} = \int \frac{d\hat{\mathbf{\Omega}}}{4\pi} \left(\frac{T}{|1 - \rho e^{2ikR}|^2} \cos^2(k\hat{\mathbf{\Omega}} \cdot \mathbf{r}) \right.$$

$$\left. + \frac{T}{|1 + \rho e^{2ikR}|^2} \sin^2(k\hat{\mathbf{\Omega}} \cdot \mathbf{r}) \right) \quad (65)$$

and propose the following interpretation: through the center of the cavity we may draw a ray in any direction; that ray reflects on the inner face of the cavity back onto itself and gives rise to a system of stationary waves. For any such ray, the field oscillations (forced by the outside vacuum) may have maximum amplitude or a node at the center: correspondingly, the stationary wave will have squared amplitude $\cos^2(k\hat{\mathbf{\Omega}} \cdot \mathbf{r})$ or $\sin^2(k\hat{\mathbf{\Omega}} \cdot \mathbf{r})$ at the point of interest.

As for the contribution of rays that support a mode having an antinode at the cavity center, they have different phases away from the origin according to their direction and thus contribute in the average with weight $1/2$: the former considerations on the positions of nodes of Bessel functions are now reformulated as positions of nodes of stationary waves along rays with different directions.

Spherical aberrations

As it can be seen in Figure 2, the simple ray-optics analysis described above agrees approximately with the results of the operator-based numerical computation in the vicinity of the center, but fails to describe the vacuum fluctuations away from that area.

Indeed, in order to handle field properties at a point located at a distance r form the origin, we shall not consider anymore the effect of rays going through the origin, but rather that of rays going through this point: such rays miss the origin by a distance $d < r$, and thus carry $\ell < kr$

orbital momentum in $\hbar$ units. These rays do not close after one round trip: if we do not move too far from the origin, we may still assume that any point is imaged onto its symmetric after one reflection, and so onto itself after two reflections, but the (twice) reflected way is tilted by an angle $\delta\theta = (4r/R)\sin\theta$. However, as we are considering finesse values in the range 10–100, and r, R values respectively smaller than 10^2 and $10^5 \lambdabar$, we may reasonably neglect this tilt and and associate to any ray an average value θ. Note that θ corresponds to ℓ via $\ell = kr\sin\theta$. Since ℓ is conserved at reflection on the mirror, due to the symmetry with respect to a radius, the change in the direction of the light ray is actually accompanied by a lack of re-imaging of the point back to itself. So, our assumption really consists in neglecting both the tilt and the lack of re-imaging, and correspondingly in keeping the spatial modulation $\cos^2 kr$ and $\sin^2 kr$ in the expressions given above.

What cannot be neglected, however, is the relative phase with which the reflected light comes back to the initial point: for off-center rays, a round trip involves propagation on a distance $4R + (2r^2/R)\sin^2\theta$. Consequently, the frequency-dependent factor acquire an extra phase term and becomes $2ikR + (ikr^2/R)\sin^2\theta$. As it can be seen in Figure 3, this phase term is basically responsible for the decrease of the spectral density as a function of the distance.

Boundary effects and diffraction losses

The formulation in terms of light rays described above can be straightforwardly extended from a closed to an open cavity: to any ray we associate an enhancement factor, which is frequency-dependent if the ray meets the mirror, and is unity if the ray misses the mirror, as well as a spatially-dependent term describing the intensity modulation of the stationary waves.

When the two mirrors are identical, we use the results known for symmetrical Fabry-Perot resonators and
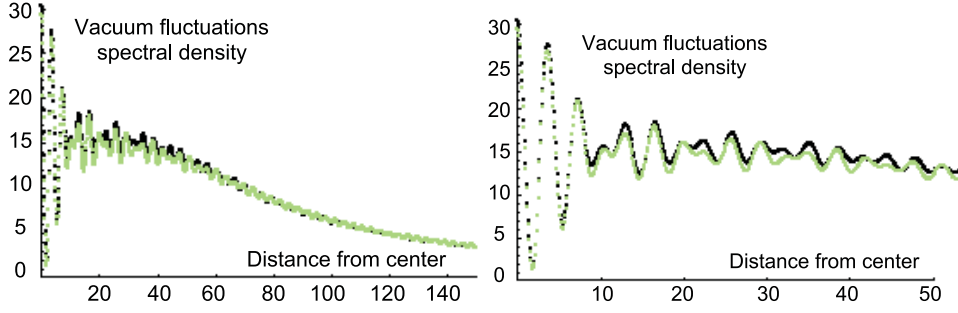
Fig. 3. Same as Figure 2, now including spherical aberrations, so that the spectral density is now decreasing as a function of the distance. The result of the full calculation (Fig. 1) is shown for comparison.
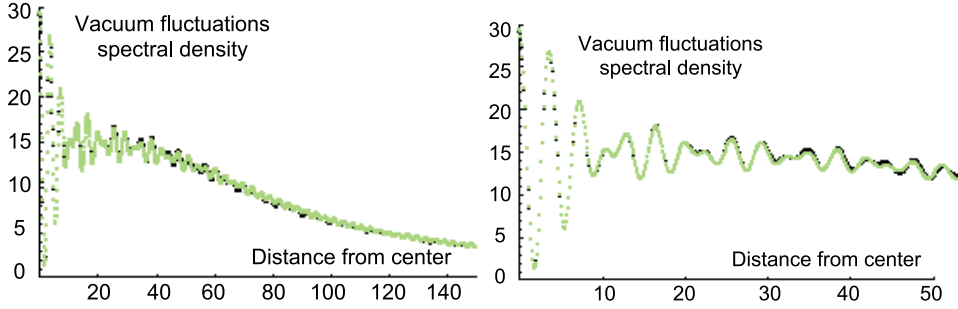
Fig. 4. Same as Figure 2, now including both spherical aberrations and diffraction losses. The result is now in very good agreement with the full calculation (Fig. 1), which is also shown for comparison.

obtain:

$$\frac{\left\langle |\phi(\mathbf{r})|^2 \right\rangle_{\mathrm{cav}}}{\left\langle |\phi(\mathbf{r})|^2 \right\rangle_{\mathrm{vac}}} =$$

$$\int \frac{d\hat{\mathbf{\Omega}}}{4\pi} \left(\frac{T}{\left| 1 - \rho e^{2ikR} e^{i\frac{kr^2}{R}\sin^2\theta} \right|^2} \cos^2(k\hat{\mathbf{\Omega}}\cdot\mathbf{r}) \right.$$

$$\left. + \frac{T}{\left| 1 + \rho e^{2ikR} e^{i\frac{kr^2}{R}\sin^2\theta} \right|^2} \sin^2(k\hat{\mathbf{\Omega}}\cdot\mathbf{r}) \right). \quad (66)$$

Should the two mirrors be different, the formula would be easily modified, just as in the case of a usual Fabry-Perot resonator (see Appendix A). In particular, the maximal enhancement at the center of a symmetrical cavity subtending a total solid angle Ω_m is:

$$\frac{\left\langle |\phi(0)|^2 \right\rangle_{\mathrm{cav}}}{\left\langle |\phi(0)|^2 \right\rangle_{\mathrm{vac}}} = \frac{\Omega_{\mathrm{vac}}}{4\pi} + \frac{T}{|1-\rho|^2}\frac{\Omega_m}{4\pi}. \quad (67)$$

It is worth noting that the ray-formula without spherical aberrations given above corresponds exactly to the result of the more rigourous analysis, when one neglects Δ_S, i.e., if one takes $e^{i\Delta_S/kR}$ equal to unity. Though the main effect of Δ_S is accounted for by spherical aberrations, a small

discrepancy remains: for $\rho_m = 0.98$ and $\Omega_m/4\pi = 0.3$, the numerical computation in the basis of spherical harmonics yields an enhancement factor of 29.2 at the cavity center and at resonance, while the ray computation gives 30.4 in the same conditions. We shall explain this small difference by diffraction losses: those rays that would be reflected near the edge of the mirror are actually lost due to diffraction and fail to do as many round-trips as the other rays. This second effect of Δ_S can be estimated by looking for an approximate inverse of the operator $(e^{i\frac{\Delta_S}{kR}} - \rho(\theta))$, valid near the mirror edge. The result of this procedure is that one can still use the previous formula for any detuning and at any point, provided that the boundary value θ_m is decreased to $\theta_{\mathrm{eff}} = \theta_m - \delta\theta$, with $\delta\theta = 1/\sqrt{kRT}$ for symmetrical mirrors, and $\delta\theta = 1/\sqrt{kR(1-\rho_{\mathrm{av}}^2)}$ for non-symmetrical mirrors, ρ_{av} being the average reflectivity $(\rho_1+\rho_2)/2$ of the two mirrors. Applying this procedure to the above example, we shall substract

$$\frac{1}{\sqrt{kRT}}\sin(\theta_m)\left(\frac{T}{|1-\rho|^2} - 1 \right) = 1.2, \quad (68)$$

which is quite satisfactory since $30.4 - 1.2 = 29.2$.

The comparison of the ray calculation and of the complete one for an open cavity is shown in Figure 4, with the same parameters as for Figure 1. As it can be seen, the agreement is very good, and justifies a posteriori the assumptions which have been made. It can therefore be concluded that the main correction to the naive calculation is the phase error due to spherical aberrations,

with some small correction from the edge diffraction losses. These corrections are enough to get the right answer in the conditions that we are considering ($R \sim 10^5 \lambda$, r smaller than 100λ).

Focusing defects

The numerical scheme of the previous sections allows us to systematically study the effects of mechanical defects in the cavity, e.g. defocusing, or non perfectly spherical mirrors. For instance, one can reproduce an axial mispositioning of the mirrors by a length δ, by adding an imaginary part to the mirror reflectivity: $\rho(\theta) = \rho_0 e^{2ik\sqrt{R^2+\delta^2+2R\delta\cos\theta}-R} = \rho_0 e^{2ik\delta\cos\theta}$. The first effect of such a mispositioning is to shift the resonance frequency. Correcting for this shift, the second effect is to decrease the enhancement effect, which is typically halved for $\delta = 40$ nm ($k\delta = 0.3$) with the previous parameters. Here again, it can be seen that the ray formula gives the right answer. As it was discussed above for positions outside the cavity center, the main feature is indeed the phase shift after one reflection, which is correctly described by the modified value of $\rho(\theta)$, while the tilting and non-imaging effect can be neglected.

2.3 Polarization effects

The above considerations, which were done for a scalar field, can be straightforwardly extended to the case of a vector field, which is needed to describe polarization effects. Here we will skip the explicit operatorial formulas, and give only the results obtained in the ray optics approximation. As previously, this approximate solution was checked by comparison with the complete numerical calculation, and found to be in complete agreement with it. For a transverse vector field $\phi(\mathbf{r})$ and for two polarization directions $\boldsymbol{\epsilon}_1$ and $\boldsymbol{\epsilon}_2$, the results obtained in the scalar case (Eq. (66)) are then changed into:

$$
\frac{\langle (\boldsymbol{\epsilon}_1 \cdot \phi(\mathbf{r}))^* \times (\boldsymbol{\epsilon}_2 \cdot \phi(\mathbf{r})) \rangle_{\text{cav}}}{\langle (\boldsymbol{\epsilon}_1 \cdot \phi(\mathbf{r}))^* \times (\boldsymbol{\epsilon}_1 \cdot \phi(\mathbf{r})) \rangle_{\text{vac}}} =
$$
$$
\int \frac{d\hat{\boldsymbol{\Omega}}}{4\pi} \frac{3}{2} \left(\boldsymbol{\epsilon}_1 \cdot \boldsymbol{\epsilon}_2 - (\hat{\boldsymbol{\Omega}} \cdot \boldsymbol{\epsilon}_1)(\hat{\boldsymbol{\Omega}} \cdot \boldsymbol{\epsilon}_2) \right)
$$
$$
\times \left(\frac{T}{|1 - \rho e^{2i\phi}|^2} \cos^2(k\hat{\boldsymbol{\Omega}} \cdot \mathbf{r}) \right.
$$
$$
\left. + \frac{T}{|1 + \rho e^{2i\phi}|^2} \sin^2(k\hat{\boldsymbol{\Omega}} \cdot \mathbf{r}) \right). \quad (69)
$$

From this equation, the cavity induced damping and level shifts can be obtained using equations (1) and (2) by integration over the frequency, which is straightforward for the damping, and requires contour integration for the level shifts (see Appendix B). Finally, the effect of the cavity can be described to a very good approximation by the

following formulas:

$$
\frac{\Gamma(\mathbf{r})}{\Gamma_{\text{vac}}} = \int_{4\pi} \frac{d\hat{\boldsymbol{\Omega}}}{4\pi} \frac{3}{2} \left(1 - \left(\frac{\mathbf{d} \cdot \hat{\boldsymbol{\Omega}}}{d} \right)^2 \right)
$$
$$
\times \left(\frac{T}{|1 - \rho e^{2i\phi}|^2} \cos^2(k\hat{\boldsymbol{\Omega}} \cdot \mathbf{r}) + \frac{T}{|1 + \rho e^{2i\phi}|^2} \sin^2(k\hat{\boldsymbol{\Omega}} \cdot \mathbf{r}) \right)
$$
$$
\tag{70}
$$

$$
\frac{\Delta'(\mathbf{r})}{\Gamma_{\text{vac}}} = \int_{4\pi} \frac{d\hat{\boldsymbol{\Omega}}}{4\pi} \frac{3}{2} \left(1 - \left(\frac{\mathbf{d} \cdot \hat{\boldsymbol{\Omega}}}{d} \right)^2 \right)
$$
$$
\times \left(\frac{\rho \sin(2\phi)}{|1 - \rho e^{2i\phi}|^2} \cos^2(k\hat{\boldsymbol{\Omega}} \cdot \mathbf{r}) - \frac{\rho \sin(2\phi)}{|1 + \rho e^{2i\phi}|^2} \sin^2(k\hat{\boldsymbol{\Omega}} \cdot \mathbf{r}) \right)
$$
$$
\tag{71}
$$

where the notation $\hat{\boldsymbol{\Omega}}$ describes a direction in space, while ϕ is a cavity detuning parameter that will be detailed below. As previously, these expressions have a straightforward interpretation, because they appear basically as integrals over the direction of light rays: in the integral over the directions, ρ is the mirror reflectivity for rays subtended by the cavity, and is zero for rays outside the cavity solid angle. The different factors appearing in the integrals are detailed below.

The first factor under the integral corresponds to polarisation effects, taking into account the transverse character of the field.

The second (resonance) factor is of the usual Fabry-Perot form, where ϕ is the cavity phase shift which includes first a term $\phi_0 = \omega_0 R/c$. As it was shown before, in order to obtain a correct result outside the cavity center, ϕ must include also a contribution from spherical aberrations, that is: $\phi = \phi_0 + k(r^2 - (\hat{\boldsymbol{\Omega}} \cdot \mathbf{r})^2)/2R$. This second term corresponds to the extra phase shift experienced by rays going through point $\mathbf{r}$ while propagating along the $\hat{\boldsymbol{\Omega}}$-direction. The resonance factor has obviously different expressions for the damping and the lamb shift terms, which correspond respectively to the active and reactive parts of the coupling. This is clearly apparent from the integrals of equations (1) and (2), which involve either a delta function or a principal part. In the first case, the integration is trivial, and yields the resonance term of equation (70), while in the second case the result is obtained by contour integration, and gives the "dispersive" second term of equation (71).

The third term under the integrals is the stationary wave pattern corresponding either to odd modes (which have an anti-node in the center and a $\cos^2(k\hat{\boldsymbol{\Omega}} \cdot \mathbf{r})$ space dependence) or to even modes (which have a node in the center and a $\sin^2(k\hat{\boldsymbol{\Omega}} \cdot \mathbf{r})$ space dependence).

Finally, the integration over the mirrors is conveniently performed in spherical coordinates, by taking the z-axis along the cavity axis, and varying the azimuthal angle θ from 0 to $\theta_{\text{mirror}} = \theta_m$. Improved accuracy (better than 1%) is obtained if one takes into account the fact
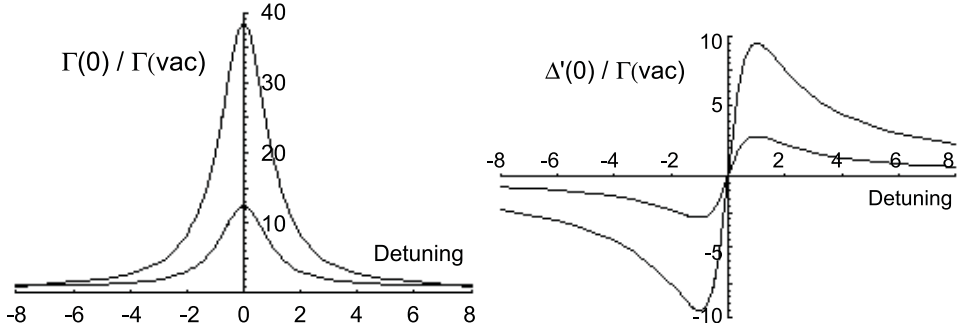
Fig. 5. Normalized damping $\Gamma(0)/\Gamma_{\mathrm{vac}}$ (left) and level shift $\Delta'(0)/\Gamma_{\mathrm{vac}}$ (right) at the cavity center, as a function of the atom-cavity detuning normalized to the cavity linewidth. The amplitude reflection coefficient of the mirrors is taken to be $\rho = 0.98$, and the numerical aperture of the cavity is 0.7. The upper curves correspond to a dipole oriented perpendicular to the cavity axis, and the lower curves to a dipole oriented along the cavity axis.

that the rays which would be reflected near the edge of the mirror are actually lost due to diffraction and fail to do as many round-trips as the other ones. As before, this effect can be taken into account very simply by decreasing θ_m to $\theta_{eff} = \theta_m - \delta\theta$, with $\delta\theta = 1/\sqrt{kRT}$ for symmetrical mirrors.

The first results which can be obtained from the previous formulas are obviously the shift and damping at the cavity center, as a function of the atom-cavity detuning. For a dipole orientation parallel to the cavity axis, we obtain straightforwardly:

$$\frac{\Gamma_{\mathrm{par}}(\mathbf{0})}{\Gamma_{\mathrm{vac}}} = \frac{\Delta\Omega_{\mathrm{vac}}}{4\pi}\left(1 + \frac{\sin^2\theta_m}{2}\right)$$
$$+ \frac{\Delta\Omega_{\mathrm{cav}}}{4\pi}\left(1 - \frac{\cos\theta_m\,(1+\cos\theta_m)}{2}\right)\frac{T}{|1 - \rho e^{2i\phi_0}|^2} \quad (72)$$

$$\frac{\Delta'_{\mathrm{par}}(\mathbf{0})}{\Gamma_{\mathrm{vac}}} =$$
$$\frac{\Delta\Omega_{\mathrm{cav}}}{4\pi}\left(1 - \frac{\cos\theta_m\,(1+\cos\theta_m)}{2}\right)\frac{\rho\,\sin(2\phi_0)}{|1 - \rho e^{2i\phi_0}|^2} \quad (73)$$

while for a dipole orientation perpendicular to the cavity axis, we have:

$$\frac{\Gamma_{\mathrm{perp}}(\mathbf{0})}{\Gamma_{\mathrm{vac}}} = \frac{\Delta\Omega_{\mathrm{vac}}}{4\pi}\left(1 - \frac{\sin^2\theta_m}{4}\right)$$
$$+ \frac{\Delta\Omega_{\mathrm{cav}}}{4\pi}\left(1 + \frac{\cos\theta_m\,(1+\cos\theta_m)}{4}\right)\frac{T}{|1 - \rho e^{2i\phi_0}|^2} \quad (74)$$

$$\frac{\Delta'_{\mathrm{perp}}(\mathbf{0})}{\Gamma_{\mathrm{vac}}} =$$
$$\frac{\Delta\Omega_{\mathrm{cav}}}{4\pi}\left(1 + \frac{\cos\theta_m\,(1+\cos\theta_m)}{4}\right)\frac{\rho\,\sin(2\phi_0)}{|1 - \rho e^{2i\phi_0}|^2}. \quad (75)$$

We note that these expressions yield for a randomly oriented dipole:

$$\frac{\Gamma_{\mathrm{av}}(\mathbf{0})}{\Gamma_{\mathrm{vac}}} = \frac{\Delta\Omega_{\mathrm{vac}}}{4\pi} + \frac{\Delta\Omega_{\mathrm{cav}}}{4\pi}\frac{T}{|1 - \rho e^{2i\phi_0}|^2},$$
$$\frac{\Delta'(\mathbf{0})}{\Gamma_{\mathrm{vac}}} = \frac{\Delta\Omega_{\mathrm{cav}}}{4\pi}\frac{\rho\,\sin(2\phi_0)}{|1 - \rho e^{2i\phi_0}|^2} \quad (76)$$

corresponding to the scalar case already given above. We note that these results are the same as those given in reference [7], up to factor two resulting from the fact that this reference was considering spatially averaged values rather than the peak value at the cavity center (see below for the space dependence). These functions are plotted in Figure 5 for $\Omega_{\mathrm{cav}}/4\pi = 0.3$ and $\rho = 0.98$. It can be seen that very significant effects occur for these quite reasonable parameters, yielding more than 30-fold increase in the damping rate at the cavity center.

The above formulas also give the damping and level shifts as a function of space for a given frequency, which are an important result of the present paper. The results in the most general case where the two mirrors have different reflectivities are given in Appendix C. Two atom-cavity detunings are specially worth looking at: the resonant frequency at the cavity center, which yields maximum change in the damping rate but no cavity shift, and frequencies detuned by plus or minus half a cavity linewidth, which yield maximum cavity shifts. These results will be exploited in the following paper [13], which deals with vacuum-induced light forces acting on an atom close to the cavity center.

3 Conclusion

As a conclusion, we have calculated explicitly the cavity induced damping and level shifts for an atomic dipole close to the center of a spherical cavity. Our results are valid for arbitrary (large) aperture and (not too large) mirrors reflectivities (for the most general case see Appendix C). These results show that macroscopic cavities with large

$$M = \frac{2\left(\tau_1^2 + \tau_2^2\right)\left(\cos^2(\phi)\cos^2(k\hat{\mathbf{\Omega}}\cdot\mathbf{r}) + \sin^2(\phi)\sin^2(k\hat{\mathbf{\Omega}}\cdot\mathbf{r})\right) + \left(\tau_1^2 - \tau_2^2\right)\sin(2\phi)\sin(2\,k\hat{\mathbf{\Omega}}\cdot\mathbf{r})}{\left(e^{4\,i\,\phi} - 1 + (\tau_1^2 + \tau_2^2)/2\right)\left(e^{-4\,i\,\phi} - 1 + (\tau_1^2 + \tau_2^2)/2\right)} \tag{81}$$

numerical apertures are interesting candidates for cavity QED experiments in the optical domain. In particular, we show in a joint paper [13] that the cavity-induced level shifts are responsible for a "vacuum-field" force on at atom moving close to the cavity center [14,15]. An explicit expression of the trapping potential can be obtained from the results given above.

Appendix A

When the mirrors' transmission are different, equation (66) can be generalized to:

$$\frac{\left\langle|\phi(\mathbf{r})|^2\right\rangle_{\text{cav}}}{\left\langle|\phi(\mathbf{r})|^2\right\rangle_{\text{vac}}} = $$

$$\int \frac{d\hat{\mathbf{\Omega}}}{4\pi}\, M\left(\mathbf{r}, \phi = kR + \frac{k\left(r^2 - (\hat{\mathbf{\Omega}}\cdot\mathbf{r})^2\right)}{2R}\right) \tag{77}$$

where $r = |\,\mathbf{r}\,|$, and:

$$M = \frac{\tau_1{}^2\left(1 + \rho_2{}^2 + 2\rho_2\cos\left(2\left(\phi - k\hat{\mathbf{\Omega}}\cdot\mathbf{r}\right)\right)\right)}{2\left(1 - e^{-4\,i\,\phi}\rho_1\rho_2\right)\left(1 - e^{4\,i\,\phi}\rho_1\rho_2\right)}$$
$$+ \frac{\tau_2{}^2\left(1 + \rho_1{}^2 + 2\rho_1\cos\left(2\left(\phi + k\hat{\mathbf{\Omega}}\cdot\mathbf{r}\right)\right)\right)}{2\left(1 - e^{-4\,i\,\phi}\rho_1\rho_2\right)\left(1 - e^{4\,i\,\phi}\rho_1\rho_2\right)} \tag{78}$$

where for each mirror $\tau_i^2 + \rho_i^2 = 1$. This equation can also be written in the less compact but more transparent form:

$$M = $$
$$\frac{(1 - \rho_1\rho_2)\left(1 + \rho_1\rho_2 + (\rho_1 + \rho_2)\cos(2\phi)\right)}{(1 - e^{-4i\phi}\rho_1\rho_2)(1 - e^{4i\phi}\rho_1\rho_2)}\cos^2(k\hat{\mathbf{\Omega}}\cdot\mathbf{r})$$
$$+ \frac{(1 - \rho_1\rho_2)\left(1 + \rho_1\rho_2 - (\rho_1 + \rho_2)\cos(2\phi)\right)}{(1 - e^{-4i\phi}\rho_1\rho_2)(1 - e^{4i\phi}\rho_1\rho_2)}\sin^2(k\hat{\mathbf{\Omega}}\cdot\mathbf{r})$$
$$+ \frac{(1 + \rho_1\rho_2)(\rho_2 - \rho_1)\sin(2\phi)}{(1 - e^{-4i\phi}\rho_1\rho_2)(1 - e^{4i\phi}\rho_1\rho_2)}\sin(2k\hat{\mathbf{\Omega}}\cdot\mathbf{r}) \tag{79}$$

which has the same interpretation as equation (66): the $\sin^2(k\hat{\mathbf{\Omega}}\cdot\mathbf{r})$ and $\cos^2(k\hat{\mathbf{\Omega}}\cdot\mathbf{r})$ correspond to the contributions of the in-phase and out-of-phase standing waves along the direction $\hat{\mathbf{\Omega}}$, while $\sin(2k\hat{\mathbf{\Omega}}\cdot\mathbf{r}) = 2\sin(k\hat{\mathbf{\Omega}}\cdot\mathbf{r})\cos(k\hat{\mathbf{\Omega}}\cdot\mathbf{r})$ is an interference term due to the intensity inbalance between the forward and backward contributions.

In the case of a high finesse cavity (τ_1, $\tau_2 \ll 1$), these equations can be rewritten:

$$M = $$
$$\frac{2\left(\tau_1^2\cos^2(\phi - k\hat{\mathbf{\Omega}}\cdot\mathbf{r}) + \tau_2^2\cos^2(\phi + k\hat{\mathbf{\Omega}}\cdot\mathbf{r})\right)}{\left(e^{4i\phi} - 1 + \left(\tau_1^2 + \tau_2^2\right)/2\right)\left(e^{-4i\phi} - 1 + \left(\tau_1^2 + \tau_2^2\right)/2\right)} \tag{80}$$

or alternatively:

see equation (81) above.

For a symmetrical high-finesse cavity with $\tau_1 = \tau_2 = \tau$, one obtains finally:

$$M = \frac{4\tau^2(\cos^2(\phi)\cos^2(k\hat{\mathbf{\Omega}}\cdot\mathbf{r}) + \sin^2(\phi)\sin^2(k\hat{\mathbf{\Omega}}\cdot\mathbf{r}))}{(e^{4i\phi} - 1 + \tau^2)(e^{-4i\phi} - 1 + \tau^2)} \tag{82}$$

which can also be obtained directly from equation (66).

Appendix B

Let us consider the normalized Airy function:

$$\mathcal{L}(\phi) = \frac{\sqrt{1 + F}}{1 + F\sin^2\phi} = \frac{1 - \rho^2}{|1 - \rho e^{2i\phi}|^2} \tag{83}$$

where F is related to the mirrors amplitude reflectivity by $F = 4\rho/(1 - \rho)^2$. In order to calculate the level shift, we need to evaluate the principal part integral:

$$\Delta(\phi) = \int \mathcal{P}\frac{d\delta}{\delta}\,\mathcal{L}(\phi - \delta). \tag{84}$$

Replacing $\mathcal{L}(\phi - \delta)$ by its uneven part $\frac{1}{2}(\mathcal{L}(\phi - \delta) - \mathcal{L}(\phi + \delta))$, $\Delta(\phi)$ can be expressed as a standard integral:

$$\Delta(\phi) = $$
$$\frac{1}{2}\int \frac{d\delta}{\delta}\left(\frac{\sqrt{1 + F}}{1 + F\sin^2(\delta - \phi)} - \frac{\sqrt{1 + F}}{1 + F\sin^2(\delta + \phi)}\right). \tag{85}$$

This quantity can be evaluated by contour integration, using the zeros of the denominators $1 + F\sin^2(\delta \pm \phi)$, which are respectively $\delta_n^- = -\phi \pm i\beta + n\pi$, and $\delta_n^+ = \phi \pm i\beta + n\pi$, where $\beta > 0$ and $\sinh^2\beta = 1/F$. Using a contour in the lower part of the complex plane, which includes the poles $\delta_n^\pm = \pm\phi - i\beta + n\pi$ with $n = \ldots -1, 0, 1, \ldots$, we obtain for instance:

$$\int \frac{d\delta}{\delta}\frac{1}{1 + F\sin^2(\delta - \phi)} = \frac{-2i\pi}{F\sin(-2i\beta)}\,\Sigma_n\frac{1}{\phi - i\beta + n\pi}$$
$$= \frac{2\pi}{F\sinh(2\beta)}\frac{1}{\tan(\phi - i\beta)}. \tag{86}$$

Using $\sinh(2\beta) = 2\sqrt{1+F}$ and $\tan(\phi - i\beta) = \frac{\sqrt{1+F}\sin\phi - i\cos\phi}{\sqrt{1+F}\cos\phi + i\sin\phi}$, we obtain thus:

$$
\begin{aligned}
\Delta(\phi) &= \frac{\pi}{2}\left(\frac{1}{\tan(\phi - i\beta)} - \frac{1}{\tan(-\phi - i\beta)}\right) \\
&= \frac{\pi F}{2}\left(\frac{\sin(2\phi)}{1 + F\sin^2\phi}\right).
\end{aligned} \tag{87}
$$

Coming back to mirrors reflectivities, we obtain finally the expression used in equation (71):

$$
\Delta(\phi) = 2\pi\,\frac{\rho\sin(2\phi)}{|1 - \rho e^{2i\phi}|^2}. \tag{88}
$$

Appendix C

In the case of asymmetrical mirrors with amplitude transmitivities ρ_1 and ρ_2, one can use the formulas of Appendix B, changing F into $F' = 4\rho_1\rho_2/(1 - \rho_1\rho_2)^2$, and ϕ into $\phi' = 2\phi$, so that:

$$
\Delta(\phi') = \frac{\pi\,F'}{2}\left(\frac{\sin(2\phi')}{1 + F'\sin^2\phi'}\right). \tag{89}
$$

In addition, we need to evaluate the principal parts for $\mathcal{L}(\phi - \delta)$ multiplied either by $\cos(\phi - \delta)$ or $\sin(\phi - \delta)$. Taking for instance the cosine part, we obtain:

$$
\Delta_c(\phi) = \int \mathcal{P}\frac{d\delta}{\delta}\,\mathcal{L}(\phi - \delta)\,\cos(\phi - \delta). \tag{90}
$$

This can be done as before, and we have:

$$
\begin{aligned}
\int \frac{d\delta}{\delta}\frac{\cos(\delta - \phi)}{1 + F\sin^2(\delta - \phi)} &= \frac{-2i\pi}{F\sin(-2i\beta)}\,\Sigma_n\frac{\cos(-i\beta + n\pi)}{\phi - i\beta + n\pi} \\
&= \frac{2\pi}{F}\frac{\cosh(\beta)}{\sinh(2\beta)}\frac{1}{\sin(\phi - i\beta)}.
\end{aligned} \tag{91}
$$

Using $\sin(\phi - i\beta) = (\sqrt{1+F}\sin\phi - i\cos\phi)/\sqrt{F}$ we get:

$$
\begin{aligned}
\Delta_c(\phi) &= \frac{\pi\,\sqrt{F(1+F)}}{2F}\left(\frac{1}{\sin(\phi - i\beta)} - \frac{1}{\sin(-\phi - i\beta)}\right) \\
&= \pi\,(1 + F)\frac{\sin\phi}{1 + F\sin^2\phi}.
\end{aligned} \tag{92}
$$

Applying the same method for the sine part, we obtain finally:

$$
\begin{aligned}
\Delta_c(\phi') &= \pi\,(1 + F')\frac{\sin\phi'}{1 + F'\sin^2\phi'} \\
\Delta_s(\phi') &= -\pi\,\frac{\cos\phi'}{1 + F'\sin^2\phi'}.
\end{aligned} \tag{93}
$$

From these formulas, we obtain the damping and level shift in the asymmetrical case:

$$
\begin{aligned}
\frac{\Gamma(\mathbf{r})}{\Gamma_{\text{vac}}} = \int_{4\pi}\frac{d\hat{\Omega}}{4\pi}\,\frac{3}{2}&\left(1 - \left(\frac{\mathbf{d}\cdot\hat{\Omega}}{d}\right)^2\right) \\
\times\Bigg\{&\frac{(1 - \rho_1\rho_2)(1 + \rho_1\rho_2 + (\rho_1 + \rho_2)\cos(2\phi))}{(1 - e^{-4i\phi}\rho_1\rho_2)(1 - e^{4i\phi}\rho_1\rho_2)}\cos^2(k\hat{\Omega}\cdot\mathbf{r}) \\
&+ \frac{(1 - \rho_1\rho_2)(1 + \rho_1\rho_2 - (\rho_1 + \rho_2)\cos(2\phi))}{(1 - e^{-4i\phi}\rho_1\rho_2)(1 - e^{4i\phi}\rho_1\rho_2)}\sin^2(k\hat{\Omega}\cdot\mathbf{r}) \\
&+ \frac{(1 + \rho_1\rho_2)(\rho_2 - \rho_1)\sin(2\phi)}{(1 - e^{-4i\phi}\rho_1\rho_2)(1 - e^{4i\phi}\rho_1\rho_2)}\sin(2k\hat{\Omega}\cdot\mathbf{r})\Bigg\}
\end{aligned} \tag{94}
$$

$$
\begin{aligned}
\frac{\Delta'(\mathbf{r})}{\Gamma_{\text{vac}}} = \int_{4\pi}\frac{d\hat{\Omega}}{4\pi}\frac{3}{2}&\left(1 - \left(\frac{\mathbf{d}\cdot\hat{\Omega}}{d}\right)^2\right) \\
\times\Bigg\{&\frac{\rho_1\rho_2\sin(4\phi) + (\rho_1 + \rho_2)(1 + \rho_1\rho_2)\sin(2\phi)/2}{(1 - e^{-4i\phi}\rho_1\rho_2)(1 - e^{4i\phi}\rho_1\rho_2)}\cos^2(k\hat{\Omega}\cdot\mathbf{r}) \\
&+ \frac{\rho_1\rho_2\sin(4\phi) - (\rho_1 + \rho_2)(1 + \rho_1\rho_2)\sin(2\phi)/2}{(1 - e^{-4i\phi}\rho_1\rho_2)(1 - e^{4i\phi}\rho_1\rho_2)}\sin^2(k\hat{\Omega}\cdot\mathbf{r}) \\
&+ \frac{(1 - \rho_1\rho_2)(\rho_1 - \rho_2)\cos(2\phi)/2}{(1 - e^{-4i\phi}\rho_1\rho_2)(1 - e^{4i\phi}\rho_1\rho_2)}\sin(2k\hat{\Omega}\cdot\mathbf{r})\Bigg\}.
\end{aligned} \tag{95}
$$

An particularly interesting case is a one-mirror cavity ($\rho_1 = \rho$, $\rho_2 = 0$), for which

$$
\begin{aligned}
\frac{\Gamma(\mathbf{r})}{\Gamma_{\text{vac}}} = \int_{4\pi}\frac{d\hat{\Omega}}{4\pi}\,\frac{3}{2}&\left(1 - \left(\frac{\mathbf{d}\cdot\hat{\Omega}}{d}\right)^2\right) \\
&\times\left\{1 + \rho\,\cos\left(2(k\hat{\Omega}\cdot\mathbf{r} + \phi)\right)\right\}
\end{aligned} \tag{96}
$$

$$
\begin{aligned}
\frac{\Delta'(\mathbf{r})}{\Gamma_{\text{vac}}} = \int_{4\pi}\frac{d\hat{\Omega}}{4\pi}\,\frac{3}{2}&\left(1 - \left(\frac{\mathbf{d}\cdot\hat{\Omega}}{d}\right)^2\right) \\
&\times\left\{\frac{\rho}{2}\,\sin\left(2(k\hat{\Omega}\cdot\mathbf{r} + \phi)\right)\right\}.
\end{aligned} \tag{97}
$$

Neglecting spherical aberrations, one has as before $\phi = \omega_0 R/c$, while $\mathbf{r}$ corresponds to the atom's position with respect to the mirror's center of curvature. We note that these equations have the correct behaviour $\Gamma(\mathbf{r}) = \Gamma_{\text{vac}}$ and $\Delta'(\mathbf{r}) = 0$ if $\rho = 0$ (no cavity). In the case of a small solid angle $\epsilon = \Omega/(4\pi)$ subtended by the spherical mirror and a dipole orthogonal to the "cavity" axis Oz, one gets:

$$
\begin{aligned}
\frac{\Gamma(z)}{\Gamma_{\text{vac}}}\widehat{E} &\approx 1 + \frac{3\epsilon\rho}{2}\,\cos\left(2\,(kz + \phi)\right), \\
\frac{\Delta'(z)}{\Gamma_{\text{vac}}} &\approx \frac{3\epsilon\rho}{4}\,\sin\left(2\,(kz + \phi)\right).
\end{aligned} \tag{98}
$$

From equation (78), the total phase $(kz + \phi)$ corresponds to the distance l between the atom and mirror 1. Taking into account that $kz + \phi = 0$, or equivalently $kl = \pi/2\ \text{mod}\ \pi$,

are antinodes of the standing wave, one has more precisely $kl = kz + \phi + \pi/2$. Equation (98) corresponds then to the results obtained in reference [16], up to a factor $3/2$ due to the fact that the vectorial character of the dipole was ignored in reference [16]. More accurate results for any position of the atom and solid angle subtended by the mirror can be obtained from equations (96) and (97).

References

1. Bibliographic note: this paper was written in 1995, and it is presented here in its original form with minor editing. The results were initially presented by Jean-Marc Daul at the conference *Quantum Optics in Wavelength Scale Structures*, Cargèse, Corsica, August 26-September 2, 1995. The same results were also presented by Philippe Grangier at the Annual Meeting of the TMR Network *Microlasers and Cavity QED*, Les Houches, France, April 21-25, 1997
2. K.H. Drexhage, in *Progress in Optics XII*, edited by E. Wolf (North-Holland, Amsterdam, 1974)
3. D. Kleppner, Phys. Rev. Lett. **47**, 233 (1981)
4. P. Goy, J.M. Raymond, M. Gross, S. Haroche, Phys. Rev. Lett. **50**, 1903 (1983)
5. G. Gabrielse, H. Dehmelt, Phys. Rev. Lett. **55**, 67 (1985)
6. R.G. Hulet, E.S. Hilfer, D. Kleppner, Phys. Rev. Lett. **55**, 2137 (1985)
7. D.J. Heinzen, J.J. Childs, J.E. Thomas, M.S. Feld, Phys. Rev. Lett. **58**, 1320 (1987)
8. W. Jhe, A. Anderson, E.A. Hinds, D. Meschede, L. Moi, S. Haroche, Phys. Rev. Lett. **58**, 666 (1987)
9. F. De Martini, G. Innocenti, G.R. Jacobovitz, P. Mataloni, Phys. Rev. Lett. **59**, 2955 (1987)
10. Y. Zhu, A. Lezama, T.W. Mossberg, M. Lewenstein, Phys. Rev. Lett. **61**, 1946 (1988)
11. D.J. Heinzen, M.S. Feld, Phys. Rev. Lett. **59**, 2623 (1987)
12. S.E. Morin, C.C. Yu, T.W. Mossberg, Phys. Rev. Lett. **73**, 1489 (1994)
13. J.-M. Daul, P. Grangier, Eur. Phys. J. D **32**, 195 (2005)
14. S. Haroche, M. Brune, J.M. Raimond, Europhys. Lett. **14**, 19 (1991)
15. B.-G. Englert, J. Schwinger, A.O. Barut, M.O. Scully, Europhys. Lett. **14**, 25 (1991)
16. U. Dorner, P. Zoller, Phys. Rev. A **66**, 023816 (2002)